Letter

Spin-valley Silin modes in graphene with substrate-induced spin-orbit coupling

Zachary M. Raines,[1] Dmitrii L. Maslov,[2] and Leonid I. Glazman[1]
[1]*Department of Physics, Yale University, New Haven, Connecticut 06520, USA*
[2]*Department of Physics, University of Florida, Gainesville, Florida 32611, USA*

(Received 16 July 2021; revised 18 April 2022; accepted 19 April 2022; published 2 May 2022)

In the presence of an external magnetic field the Fermi-liquid state supports oscillatory spin modes known as Silin modes. We predict the existence of the generalized Silin modes in a multivalley system, monolayer graphene. A gauge- and Berry-gauge-invariant kinetic equation for a multivalley Fermi liquid is developed and applied to the case of graphene with extrinsic spin-orbit coupling (SOC). The interplay of SOC and Berry curvature allows for the excitation of generalized Silin modes in the spin and valley-staggered-spin channels via an AC electric field. The resonant contributions from these modes to the optical conductivity are calculated.

DOI: 10.1103/PhysRevB.105.L201201

It has long been known that whereas spin waves in a Fermi liquid are normally overdamped [1], in the presence of a finite Zeeman field (a magnetic field acting only on particle spins), there exist well-defined gapped spin collective modes of the Fermi-liquid state, the Silin modes [2–7]. In multivalley materials there may be additional collective excitations of the Fermi-liquid state, beyond the charge and spin modes. These additional modes are, in general, also diffusive in the time-reversal symmetric case [8]. However, in a finite Zeeman field these modes may become oscillatory, generalizing the notion of the Silin mode. The aim of this Letter is to identify these combined spin-valley modes in graphene and explore ways to excite them.

We predict a set of generalized Silin modes in graphene, composed of the spin-density Silin mode as well as a new valley-staggered Silin mode, which become oscillatory in a finite in-plane magnetic field. The mode frequencies differ from each other due to the difference between the corresponding Landau Fermi-liquid constants. An effective coupling of an electromagnetic wave to the new valley-staggered modes can be achieved by engaging the spin-orbit coupling (SOC) induced by a substrate, see, e.g., Ref. [9]. Additionally, as is the case for the usual Silin mode, SOC allows the generalized Silin modes to be excited by the electric field of the wave; this results in electric dipole spin resonance (EDSR) being the dominant [10–13] excitation mechanism.

We investigate the structure and frequencies of generalized Silin modes and find the corresponding resonances in the conductivity tensor. The modes differ not only by their frequency, but also by sensitivity to the polarization of the Electromagnetic wave exciting them, allowing modes of different character to be selectively excited.

We consider a graphene sheet with spin-orbit coupling induced by the substrate made, e.g., of a transition-metal dichalcogenide (TMD) [9]. In addition to SOC, the substrate, in general, also induces gaps at Dirac points in the graphene's electronic spectrum. We assume the electron density is tuned away from the charge-neutrality point, allowing us to apply the Fermi-liquid theory. The system is subject to a static in-plane magnetic-field $\mathbf{H}_0$ needed for the generalized Silin modes, and an AC-field $\mathbf{E}(t)$ probing them.

To describe the generalized Silin modes at long wavelength we augment the theory of a multivalley Fermi liquid [8,14,15] by including the effects of SOC and of the external fields. To deduce the linear response to the probe fields, we must first obtain the energy functional with extrinsic spin-orbit coupling and applied Zeeman field.

Model. In the presence of extrinsic spin-orbit coupling, the single-particle Dirac Hamiltonian written in the valley-sublattice basis (KA, KB, $K'B$, $-K'A$) takes the form

$$\hat{H}_{\mathbf{p}} = v_D \mathbf{p}\cdot\hat{\boldsymbol{\Sigma}} + \Delta\hat{\Sigma}_z\hat{\tau}_z + \lambda\hat{\tau}_z\hat{\sigma}_z + \lambda_R \mathbf{e}_z\cdot(\hat{\boldsymbol{\sigma}}\times\hat{\boldsymbol{\Sigma}}). \quad (1)$$

Here $\hat{\boldsymbol{\Sigma}}$, $\hat{\boldsymbol{\tau}}$, and $\hat{\boldsymbol{\sigma}}$ are the vectors of Pauli matrices in the spaces of sublattices (A, B), points K, K' in the Brillouin zone, and electron spin, respectively, and $\mathbf{e}_z$ is the unit vector in the z (out-of-plane) direction. In the absence of SOC, the graphene spectrum is characterized by the Dirac velocity v_D and gap Δ; the valley-Zeeman (λ) and Rashba (λ_R) spin-orbit couplings arise from the inversion symmetry breaking by and wave-function hybridization with the TMD substrate [9]. For definiteness, we take the Fermi level to be in the upper band. If the SOC couplings are small compared to the Fermi energy (as measured from charged neutrality), we may perform the projection onto the upper band perturbatively in λ_R and λ, obtaining the effective single band Hamiltonian (see the Supplemental Material in Ref. [16] for details),

$$\hat{H}^{+}_{\mathbf{p}} = \epsilon_{\mathbf{p}} - \tfrac{1}{2}\mu_s\mathbf{H}_0\cdot\hat{\boldsymbol{\sigma}} + \alpha_R(p)(\mathbf{p}\times\mathbf{e}_z)\cdot\hat{\boldsymbol{\sigma}} + \Lambda(p)\hat{\sigma}_z\hat{\tau}_z, \quad (2)$$

with $\epsilon_{\mathbf{p}} = \sqrt{v_D^2p^2+\Delta^2}$ being the massive Dirac dispersion, $\alpha_R(p) = v_D\lambda_R/\epsilon_{\mathbf{p}}$ the effective Rashba coupling, $\Lambda(p) = \lambda - \lambda_R^2\Delta/\epsilon_{\mathbf{p}}^2$ the effective valley-Zeeman coupling, and where we have included the Zeeman energy due to external magnetic-field $\mathbf{H}_0$ for particles with effective Bohr magneton $\mu_s = g_s e/4m_e c$, where g_s is the Landé factor and m_e is the free-electron mass. A complete description of the dynamics of the

projected upper band also requires the evaluation of the Berry connection $\hat{\boldsymbol{\mathcal{A}}}$, which consists of Abelian and non-Abelian parts [17,18]. To leading order in the Rashba term, we find $\hat{\boldsymbol{\mathcal{A}}} = \hat{\boldsymbol{\mathcal{A}}}_0 + \hat{\boldsymbol{\mathcal{A}}}_1 + O(\alpha_R^3)$, where $\hat{\boldsymbol{\mathcal{A}}}_0$ is the Abelian Berry connection of gapped graphene, whereas the non-Abelian part is given by

$$\hat{\boldsymbol{\mathcal{A}}}_1 = -\tilde{\alpha}_R(p) 2\pi \nu(\epsilon_{\mathbf{p}}) |\Omega_0^z(p)| \hat{\boldsymbol{\sigma}}_\parallel \hat{\tau}_z. \tag{3}$$

Here, $\boldsymbol{\Omega} = \Omega_0^z \mathbf{e}_z$ is the Berry curvature of gapped graphene, $\Omega_0^z(p) = \mp v_D^2 \Delta / 2\epsilon_{\mathbf{p}}^3$ with $\mp$ corresponding to the K (K') point, $\nu(\epsilon) = \epsilon / 2\pi v_D^2$ is the density of states of the graphene bands [1], and $\hat{\boldsymbol{\sigma}}_\parallel = \hat{\sigma}_x \hat{x} + \hat{\sigma}_y \hat{y}$. The tilde on $\tilde{\alpha}_R$ indicates renormalization of the effective Rashba strength which will be discussed below. The valley-Zeeman term by itself does not give rise to a non-Abelian Berry connection because it commutes with the Dirac part of the Hamiltonian.

With Eqs. (2) and (3) we are able to write a kinetic equation for the projected upper band in the collisionless limit [19],

$$\partial_t \hat{\rho} + \tfrac{1}{2}\{\boldsymbol{\nabla}\hat{\rho}; \hat{\mathbf{v}}\} + \tfrac{1}{2}\{\boldsymbol{\mathcal{D}}\hat{\rho}; \hat{\boldsymbol{F}}\} + i[\hat{\epsilon}, \hat{\rho}] = 0, \tag{4}$$

where $\hat{\rho}$ is the density matrix, $\hat{\epsilon}$ is the (matrix) quasiparticle energy functional, $\hat{\boldsymbol{F}}$ is the total force (external plus self-consistent) acting on a quasiparticle, and the Berry covariant derivative is defined as [17,18]

$$\boldsymbol{\mathcal{D}}\hat{g} = \nabla^{(\mathbf{p})}\hat{g} - \imath[\hat{\boldsymbol{\mathcal{A}}}, \hat{g}], \tag{5}$$

with $\nabla^{(\mathbf{p})}$ denoting the gradient in momentum space. The velocity and force appearing in Eq. (4) are governed by the quasiclassical equations of motion for the band [18,19]. As we are working in the two-dimensional limit, the non-Abelian Berry connection $\boldsymbol{\mathcal{A}}$ is completely in plane, whereas the non-Abelian Berry curvature $\boldsymbol{\Omega}$ is entirely out of plane. Here, we will take $\mathbf{E}, \mathbf{H}_0$ to be in plane, allowing the force and velocity terms to be simply written as

$$\hat{\mathbf{v}} \approx \boldsymbol{\mathcal{D}}\hat{\epsilon}, \quad \hat{\boldsymbol{F}} \approx e\boldsymbol{E} - \boldsymbol{\nabla}\hat{\epsilon}. \tag{6}$$

Here we have noted that in Eq. (4) $\mathbf{v}$ multiplies $\boldsymbol{\nabla}\hat{\rho}$. The latter appears in first order in $\mathbf{E}$, so within the linear-response theory we can neglect terms of order $\mathbf{E}$ in $\mathbf{v}$.

The system of Eqs. (4) and (6) provides a gauge- and Berry-gauge-invariant description of the dynamics of the system. As such, it is a convenient launching point to incorporate the interplay among band topology, spin-orbit coupling, and Fermi-liquid effects.

The quasiparticle energy functional is found by combining Eq. (2) with the interactions allowed by the approximate $SU(2)$ spin and $U(1)$ valley symmetries of gapped graphene [8,14,15],

$$\hat{\epsilon}_{\mathrm{FL}}[\hat{\rho}_{\mathbf{p}}] = \sum_{\mathbf{p}'} \big[f^d_{\mathbf{p}\mathbf{p}'} n_{\mathbf{p}'} + f^s_{\mathbf{p}\mathbf{p}'} \mathbf{s}_{\mathbf{p}'} \cdot \hat{\boldsymbol{\sigma}} + f^{v\parallel}_{\mathbf{p}\mathbf{p}'} \mathbf{Y}_{\mathbf{p}'} \cdot \hat{\boldsymbol{\tau}}_\parallel + f^{vz}_{\mathbf{p}\mathbf{p}'} Y^z_{\mathbf{p}'} \hat{\tau}_z + f^{m\parallel}_{\mathbf{p}\mathbf{p}'} \mathbf{M}^i_{\mathbf{p}'} \cdot \hat{\boldsymbol{\sigma}} \hat{\tau}_{\parallel,i} + f^{mz}_{\mathbf{p}\mathbf{p}'} \mathbf{M}^z_{\mathbf{p}'} \cdot \hat{\boldsymbol{\sigma}} \hat{\tau}_z \big], \tag{7}$$

where $\hat{\tau}_{\parallel,i}$ are the $\hat{\tau}_x$ and $\hat{\tau}_y$ components of $\hat{\boldsymbol{\tau}}$, and index i is summed over $i = x, y$. Here we have decomposed the density matrix in terms of symmetry distinguished channels,

$$\hat{\rho}_{\mathbf{p}} = n_{\mathbf{p}} + \mathbf{s}_{\mathbf{p}} \cdot \hat{\boldsymbol{\sigma}} + \mathbf{Y}_{\mathbf{p}} \cdot \hat{\boldsymbol{\tau}} + \mathbf{M}^i_{\mathbf{p}} \cdot \hat{\boldsymbol{\sigma}} \hat{\tau}_i, \tag{8}$$

and $f^\mu_{\mathbf{p}\mathbf{p}'}$ are the Landau-Fermi-liquid interaction functions associated with the channel. The collective variables in Eq. (8) are the densities of: charge n, spin $\mathbf{s}$, valley pseudospin $\mathbf{Y}$, and spin-triplet valley pseudospin $\mathbf{M}^i$.

Before considering the collective modes, we must identify the equilibrium density matrix. The equilibrium occupations in the spin and valley-spin channels are due to the presence of the external Zeeman field and Rashba coupling for the former and valley-Zeeman coupling for the latter. We consider the case where the thermal, spin-orbit and magnetic energy scales are small compared to the Fermi energy with respect to the band edge, $T, \mu_s H_0, \lambda, \lambda_R \ll E_F - \Delta$. In direct analogy with the standard computation of the spin magnetic moment of the Fermi liquid [20,21], the equilibrium density matrix is given by Eq. (8) with [16]

$$\begin{aligned} n_{\mathrm{eq},\mathbf{p}} &= n_F(\tilde{\epsilon}_{\mathbf{p}}), \qquad Y_{\mathrm{eq},\mathbf{p}} = 0 \\ \mathbf{s}_{\mathrm{eq},\mathbf{p}} &= -\frac{\partial n_F}{\partial \epsilon}\left(\frac{1}{2}\tilde{\mu}_s \mathbf{H}_0 - \tilde{\alpha}_R(p)\mathbf{p} \times \mathbf{e}_z\right), \\ \mathbf{M}^i_{\mathrm{eq},\mathbf{p}} &= \frac{\partial n_F}{\partial \epsilon} \tilde{\Lambda}(p) \mathbf{e}_z \delta_{iz}. \end{aligned} \tag{9}$$

Here, n_F is the Fermi function of the local excitation energy in the absence of SOC and magnetic field given by $\tilde{\epsilon}_{\mathbf{p}} = \epsilon_{\mathbf{p}} + \sum_{\mathbf{p}'} f^d_{\mathbf{p}\mathbf{p}'} n_F(\tilde{\epsilon}_{\mathbf{p}'})$ [2], and $\epsilon_{\mathbf{p}}$ is defined in Eq. (2). $\tilde{\mu}_s$, $\tilde{\alpha}(p)$, and $\tilde{\Lambda}(p)$ are, respectively, the renormalized by interaction effective spin magnetic moment, Rashba SOC strength [22], and valley-Zeeman SOC strength,

$$\tilde{\mu}_s = \frac{\mu_s}{1 + F_0^s}, \quad \tilde{\alpha}_R(p) = \frac{\alpha_R(p)}{1 + F_1^s}, \quad \tilde{\Lambda}(p) = \frac{\Lambda(p)}{1 + F_0^{mz}}. \tag{10}$$

The Landau Fermi-liquid parameters in Eq. (10) are

$$F_l^\mu = G_s G_v \nu_F \int \frac{d\phi}{2\pi} \frac{d\phi'}{2\pi} f^\mu(\mathbf{p}_F, \mathbf{p}'_F) e^{-il(\phi - \phi')}, \tag{11}$$

where ϕ, ϕ' are the azimuths of the respective momenta on the Fermi circles in valleys K and K' and $\mu = d, s, v\parallel, vz, m\parallel, mz$; also, ν_F is the density of states at the Fermi surface, and G_s and G_v are the spin and valley degeneracy, respectively.

Following the above considerations, we write the equilibrium energy $\hat{\epsilon}_{\mathrm{eq}} \equiv \hat{\epsilon}[\hat{\rho}_{\mathrm{eq}}]$ as

$$\hat{\epsilon}_{\mathrm{eq}} = \tilde{\epsilon}_{\mathbf{p}} - \left(\tfrac{1}{2}\tilde{\mu}_s \mathbf{H}_0 - \tilde{\alpha}_R(p)(\mathbf{p} \times \mathbf{e}_z)\right) \cdot \hat{\boldsymbol{\sigma}} + \tilde{\Lambda}\hat{\sigma}_z\hat{\tau}_z. \tag{12}$$

Linear response. To find the EDSR response of the system, we need to keep only linear-order terms in the electric field. We, thus, linearize the kinetic equation (4) in the deviation

[1] The Berry connection will only enter the collective mode equations of motion evaluated at the Fermi surface. Thus in what follows, we set $p = p_F$ and suppress the momentum arguments.

[2] Only interactions in the density channel contribute to this term as in the absence of SOC and Zeeman fields $n_{\mathbf{p}}$ is the only non-zero collective coordinate in Eq. (7).

from equilibrium $\hat{\rho} \equiv \hat{\rho}_{\rm eq} + \delta\hat{\rho}$,

$$\partial_t \delta\hat{\rho} + \tfrac{1}{2}\nabla\cdot[\{\hat{\mathbf{v}}, \delta\hat{\rho}\} - \{\delta\hat{\epsilon}, \boldsymbol{\mathcal{D}}\hat{\rho}_{\rm eq}\}] + i[\hat{\epsilon}_{\rm eq}, \delta\hat{\tilde{\rho}}] = -e\mathbf{E}\cdot\boldsymbol{\mathcal{D}}\hat{\rho}_{\rm eq}, \tag{13}$$

where we have defined the first-order correction to the quasiparticle energy from fluctuations in terms of the the Fermi-liquid interactions $\delta\hat{\epsilon} = \hat{\epsilon}_{\rm FL}[\delta\hat{\rho}]$ [cf. Eq. (7)], and the local deviation from equilibrium $\delta\hat{\tilde{\rho}} \equiv \delta\hat{\rho} - (\partial n_F/\partial\epsilon)\delta\hat{\epsilon}$.

From Eq. (13) we obtain the conductivity as follows. First, by taking the trace of Eq. (13) and integrating it over momentum, we find the continuity equation:

$$e\sum_{\mathbf{p}} \mathrm{tr}\,\partial_t\delta\hat{\rho} + \nabla\cdot e\sum_{\mathbf{p}} \mathrm{tr}(\hat{\mathbf{v}}_{\mathbf{p}}\delta\hat{\rho} - \delta\hat{\epsilon}\boldsymbol{\mathcal{D}}\hat{\rho}_{\rm eq}) = 0, \tag{14}$$

which allows us to identify the longitudinal charge current as

$$\mathbf{j} = e\sum_{\mathbf{p}} \mathrm{tr}\,(\hat{\mathbf{v}}_{\mathbf{p}}\delta\hat{\rho} - \delta\hat{\epsilon}\,\boldsymbol{\mathcal{D}}\hat{\rho}_{\rm eq}). \tag{15}$$

Using the equilibrium energy Eq. (12) and density matrix of Eq. (9) allows us to write the spin contribution to the longitudinal current (to order α_R^2 and lowest order in λ/ω_s). Expanding the dynamic variables into the angular harmonics on the Fermi surface,

$$\delta\mathbf{s}_{\mathbf{p}} = -\frac{\partial n_F}{\partial\epsilon}\sum_l \delta\tilde{\mathbf{s}}_l e^{il\phi}, \quad \delta\mathbf{M}^z_{\mathbf{p}} = -\frac{\partial n_F}{\partial\epsilon}\sum_l \delta\widetilde{\mathbf{M}}^z_l e^{il\phi}, \tag{16}$$

we write the current as [3]

$$\begin{aligned}\mathbf{j}_{\rm res} = -eG_sG_v v_F\tilde{\alpha}_R\Bigg[&\left(\frac{1}{2}\zeta + 2\pi\nu_F|\Omega_0^z|\frac{2\lambda}{\gamma_0}\right)\delta\tilde{\mathbf{s}}_0\times\mathbf{e}_z \\ &+\frac{1}{2}\left(1+F_2^s-\frac{1}{2}\zeta\right)\sum_{\pm}\pm i(\mathbf{e}_{R/L}\cdot\delta\tilde{\mathbf{s}}_{\pm2})\mathbf{e}_{R/L}\Bigg] \\ &+2\pi eG_sG_v v_F^2|\Omega_0^z|\tilde{\alpha}_R\Bigg[\frac{1+F_0^{mz}}{1+F_0^s}|\mu_s\mathbf{H}_0|\delta\widetilde{M}^z_0\mathbf{e}_y \\ &+\alpha_R p_F\left(\frac{1+F_1^s}{1+F_0^{mz}}+\frac{1}{2}\gamma_1\right)\sum_{\pm}\delta\widetilde{M}^z_{\pm1}\mathbf{e}_{R/L}\Bigg],\end{aligned} \tag{17}$$

where $\mathbf{e}_{R/L} = \mathbf{e}_x \pm i\mathbf{e}_y$ and

$$\zeta \equiv 1 + \frac{E_F - \sqrt{E_F^2 - \Delta^2}}{E_F}, \quad \gamma_l = \frac{1+F_l^{mz}}{1+F_l^s}. \tag{18}$$

Note that the presence of Ω_0^z in Eq. (17) indicates the important role of the Berry curvature in driving the valley-staggered modes (see also Fig. 1).

With an expression for the current in terms of $\delta\hat{\rho}$ we can solve the homogeneous $\mathbf{q}\to 0$ limit of Eq. (13) for $\delta\hat{\rho}$, obtaining a linear relationship between $\mathbf{j}$ and $\mathbf{E}$, and, thus, read off the dissipative part of the optical conductivity tensor.

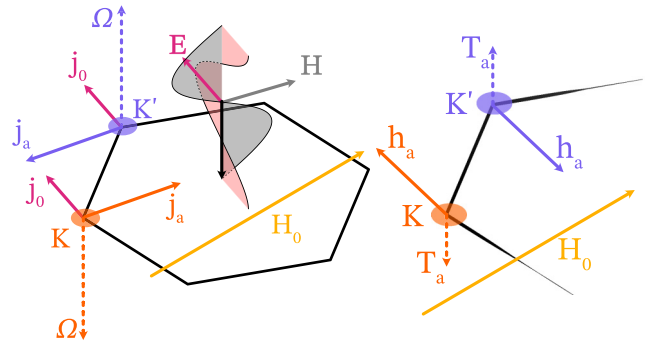

FIG. 1. Left: Electron dipole spin resonance driven by an electromagnetic wave. The regular, $\mathbf{j}_0 \propto \mathbf{E}$, and anomalous, $\mathbf{j}_a \propto \boldsymbol{\Omega}\times\mathbf{E}$, currents at the K (orange) and K' (purple) points in the Brillouin zone, induced by the electric-field $\mathbf{E}$ of the incident electromagnetic wave. Here, $\boldsymbol{\Omega}$ is the valley-staggered Berry curvature. Right: Anomalous fields and torques. Spins are initially polarized along the Zeeman field $\mathbf{H}_0$. The anomalous current-induced effective Rashba fields, $\mathbf{h}_a \propto \alpha_R\mathbf{e}_z\times\mathbf{j}_a$, produce valley-specific torques $\mathbf{T}_a \propto \mathbf{H}_0\times\mathbf{h}_a$, thus, exciting the valley-staggered spin mode with an intensity proportional to $|\mathbf{E}\times\mathbf{H}|$.

In the absence of SOC and driving, the homogeneous limit of Eq. (13) is simply

$$\partial_t\delta\hat{\rho} + i[\hat{\epsilon}_{\rm eq}, \delta\hat{\tilde{\rho}}] = 0. \tag{19}$$

In the spin and valley-spin sectors, this gives the equations [4],

$$\begin{aligned}&\partial_t\delta\tilde{\mathbf{s}}_l - \omega_{sl}\mathbf{e}_x\times\delta\tilde{\mathbf{s}}_l = 0, \quad \omega_{sl} = \frac{1+F_l^s}{1+F_0^s}|\mu_s H_0|, \\ &\partial_t\delta\widetilde{\mathbf{M}}^z_l - \omega_{ml}\mathbf{e}_x\times\delta\widetilde{\mathbf{M}}^z_l = 0, \quad \omega_{ml} = \gamma_l\omega_{sl}.\end{aligned} \tag{20}$$

Here $\delta\tilde{\mathbf{s}}$ corresponds to long-wavelength spin-density modulations, whereas $\delta\widetilde{\mathbf{M}}^z$ describes spin-density modulations on length scale $|\boldsymbol{K}-\boldsymbol{K}'|^{-1}$ corresponding to the separation between valleys in the Brillouin zone. As in the case of the conventional Silin mode [2], the mode frequencies are renormalized away from the Zeeman frequency by the Fermi-liquid parameters with the exception of the $l=0$ mode frequency, which is protected by $SU(2)$ symmetry (see Refs. [16,22,23] for how this is modified by valley-Zeeman SOC).

Conductivity resonances. Without SOC, the resonant finite frequency modes are not excited by an external electric field. However, upon introduction of the Rashba coupling, three modes may be resonantly excited, namely, the $l=0$ spin and valley-staggered spin modes, and the $l=\pm2$ spin mode. The mechanism of driving can be understood as follows. Initially, all particle spins are polarized along the external Zeeman field, which we take to be along the $\mathbf{e}_x$ axis. Upon application of an external field $\mathbf{E}(t)$ the particle spins feel an effective magnetic field due to the Rashba term $\mathbf{h}\propto\mathbf{e}_z\times\mathbf{j}$ [18,24] and, therefore, a spin torque [25,26] $\mathbf{T}\propto\mathbf{e}_x\times\mathbf{h} = \mathbf{e}_z j_x$. The

[3] As with the Berry connection Eq. (3) all functions of the magnitude of the momentum are here evaluated at $p = p_F$. We have suppressed the momentum argument of such functions for compactness, e.g. $\alpha_R = \alpha_R(p_F)$.

[4] Note we use the relations $\delta\tilde{\mathbf{s}}_l = (1+F_l^s)\delta\tilde{\mathbf{s}}_l$, $\delta\widetilde{\widetilde{\mathbf{M}}}^z_l = (1+F_l^{mz})\delta\widetilde{\mathbf{M}}^z_l$ to write Eq. (20) entirely in terms of unbarred quantities. The Fermi liquid parameters are absorbed into the definition of the mode frequencies ω_{sl}, ω_{ml}.

x component of the current j_x is composed of regular and anomalous pieces, shown in the left side of Fig. 1,

$$j_x(\omega) = -\frac{e^2 N E_x}{i\omega m^*} - e^2 N \Omega_0^z E_y, \tag{21}$$

where N is the number density, $m^* = p_F/v_F$, and $v_F = \epsilon'_{\mathbf{p}}|_{p=p_F}$. The first of these terms creates identical torques in both valleys, whereas the second one, being proportional to the Berry curvature, yields valley-staggered torques depicted in the right side of Fig. 1. Thus, the component of $\mathbf{E}$ along $\mathbf{H}_0$ causes a valley-uniform torque on the spin, exciting the spin mode, $\delta\tilde{\mathbf{s}}$, whereas the component of $\mathbf{E}$ transverse to $\mathbf{H}_0$ causes a valley-staggered torque and, thus, excites the valley-staggered spin mode $\delta\widetilde{\mathbf{M}}^z$. Because the charge-to-spin conversion in both cases is proportional to the Rashba coupling, this leads to contributions to the conductivity proportional to α_R^2. Furthermore, the $\delta\tilde{\mathbf{s}}_0$ mode contributes to σ^{xx} whereas the $\delta\widetilde{\mathbf{M}}_0^z$ mode contributes to σ^{yy}.

In the interacting case, the basic physical picture remains the same, but the quantities involved are renormalized. The resonant contributions to the dissipative part of the conductivity can be written as (see the Supplemental Material in Ref. [16])

$$\begin{aligned}
\mathrm{Re}\ \sigma_1^{ii} &= \tfrac{1}{2}\pi e^2 G_s G_v \nu_F \tilde{\alpha}_R^2 W_1^{ii} A_{m1}(\omega^2),\\
\mathrm{Re}\ \sigma_0^{ii} &= \tfrac{1}{2}\pi e^2 G_s G_v \nu_F \tilde{\alpha}_R^2 W_0^{ii} A_{s0}(\omega^2),\\
\mathrm{Re}\ \sigma_2 &= \tfrac{1}{2}\pi e^2 G_s G_v \nu_F \tilde{\alpha}_R^2 W_2 A_{s2}(\omega^2),
\end{aligned} \tag{22}$$

where $A_{\mu l}(\omega^2) \equiv \omega_{\mu l}\delta(\omega^2 - \omega_{\mu l}^2)$ is the spectral function for the relevant mode and W_l^{ii} is a dimensionless peak weight ($i = x, y$). Here the lack of indices on σ_2 indicates that the $|l| = 2$ contribution is isotropic $\sigma_2^{xx} = \sigma_2^{yy} = \sigma_2$, and it is understood that the total conductivity is the sum of the three lines in Eq. (22). Solving Eq. (13) in the homogeneous limit and substituting the result into Eq. (17) we find to order α_R^2 and without the valley-Zeeman term,

$$\begin{aligned}
&\lim_{\lambda\to 0} W_1^{ii} = 0, \quad \lim_{\lambda\to 0} W_0^{xx} = \zeta\frac{\omega_{s1}}{2\omega_{s0}},\\
&\lim_{\lambda\to 0} W_0^{yy} = \left(2\pi\nu_F\left|\Omega_0^z\right|\right)^2 \frac{\omega_{m0}^2}{1+F_0^{mz}},\\
&\lim_{\lambda\to 0} W_2 = 2\left(1+F_2^s-\frac{1}{2}\zeta\right)\left(1-\frac{\omega_{s1}}{2\omega_{s2}}\right).
\end{aligned} \tag{23}$$

Here we explicitly see that the contribution from the $l = 0$ modes has the strong anisotropy discussed above, whereas the $|l| = 2$ contribution is isotropic.

Experiment shows that valley-Zeeman coupling is generally also present [27–29]. The inclusion of the valley-Zeeman coupling causes a valley-staggered spin torque, which adds to the undriven equations of motion Eq. (20), a term coupling $\delta\tilde{\mathbf{s}}_l$ and $\delta\widetilde{\mathbf{M}}_l^z$. This leads to a modification of the weights in Eq. (23). Additionally, the valley-Zeeman term allows to excite the valley-staggered spin mode in the $|l| = 1$ channel with frequency ω_{m1}. This is simply because there is now a uniform net valley-staggered spin density [cf. Eq. (9)], thus, $|l| = 1$ deformation of the Fermi surface caused by the electric field also leads to a $|l| = 1$ modulation of valley-staggered spin [5]. To lowest nontrivial order in the valley-Zeeman coupling λ, the weights in Eq. (22) are modified to

$$\begin{aligned}
W_1^{xx} &= 2\tilde{\lambda}\left(1+F_1^s\right)2\pi\nu_F\left|\Omega_0^z\right|\\
&\quad\times\left(1+\frac{1}{2}\gamma_1^{-1}\frac{1+F_1^s}{1+F_0^{mz}}\right)(1-\gamma_1),\\
W_1^{yy} &= 2\tilde{\lambda}\left(1+F_1^s\right)2\pi\nu_F\left|\Omega_0^z\right|,\\
&\quad\times\left[\frac{\omega_{s1}-\omega_{m1}}{\omega_{m0}-\omega_{m1}}+(1-\gamma_1)\left(1+\frac{1}{2}\gamma_1^{-1}\frac{1+F_1^s}{1+F_0^{mz}}\right)\right]\\
W_0^{xx} &= \zeta\frac{\omega_{1s}}{2\omega_s}+2\tilde{\lambda}\left(2\pi\nu_F\left|\Omega_0^z\right|\right)\left(1+F_1^s-\zeta\right)\\
W_0^{yy} &= 2\pi\nu_F\left|\Omega_0^z\right|\left\{2\pi\nu_F\left|\Omega_0^z\right|\frac{\omega_{m0}^2}{1+F_0^{mz}}\right.\\
&\quad\left.+2\tilde{\lambda}\left[\left(1+F_1^{mz}\right)\frac{\omega_{s1}-\omega_{m0}}{\omega_{m0}-\omega_{m1}}-\frac{1}{1+F_0^{mz}}\zeta\right]\right\},
\end{aligned} \tag{24}$$

whereas W_2 remains unchanged. Note that there are two qualitatively different contributions to W_1. One gives W_1^{xx} and the second term in W_2^{yy} (which are identical) and comes from coupling of the $|l| = 1$ $\delta\widetilde{\mathbf{M}}^z$ mode to the $|l| = 1$ spin zero-mode $\delta\tilde{\mathbf{s}}_{l=\pm 1}$ with magnetization parallel to $\mathbf{H}_0$ via the valley-Zeeman SOC. The other term, corresponding to the first term of W_1^{yy}, arises from conversion of the $l = 0\delta\widetilde{\mathbf{M}}^z$ mode into the $|l| = 1$ mode via the Rashba SOC, which carries angular momentum 1. Both of these processes can only occur in the presence of interactions—specifically when $F_1^{mz} \neq F_1^s$ and $F_1^{mz} \neq F_0^{mz}$, respectively [6]—and arise due to the different effective magnetic moments for Zeeman vs valley-Zeeman fields.

Discussion. It should be noted that these modes may be driven as well by an AC magnetic field. Indeed, as discussed above, EDSR may be interpreted as being due to an effective Zeeman field created by the external electric field and Rashba coupling [10,13]. The relative strength of EDSR driving compared to driving by an AC magnetic field is on the order of the ratio of atomic energy scale to driving frequency $E_{\mathrm{at}}/\omega \gg 1$ [7], confirming the leading role of SOC in driving the modes [11,22].

The visibility of the generalized Silin modes in the optical conductivity will be determined by the broadening of the Silin mode peaks as well as by the extent of the Drude peak tail. In principle, this depends on two different relaxation times, the momentum relaxation time τ and spin-relaxation time τ_s. We

[5] For a more technical treatment see Ref. [16]

[6] The apparent divergence at $\omega_{m0} = \omega_{m1}$ is an artifact of the perturbation theory in λ breaking down, as it is controlled by $\lambda/(\omega_{\mu l} - \omega_{\mu' l'})$

[7] The relative strength of the magnetic driving compared to the electric driving is determined by the ratio the magnetic and electric couplings [22] $(e\alpha_R/\omega)/\mu_s = ([\{c/v_D\}\lambda_R]/\omega)(m_e v_D^2/g_s E_F)$. The SOC constant λ_R is smaller than the characteristic atomic energy scale E_{at} by the ratio of atomic velocity to speed of light, $\sim v_{\mathrm{at}}/c$. Therefore, the fraction $(c/v_D)\lambda_R/\omega$ is of the order $E_{\mathrm{at}}/\omega \gg 1$

may approximate the effect of the spin relaxation on the Silin mode peaks by broadening the δ-function peak to a Lorentzian of width τ_s^{-1}. Doing so, one may compute the ratio of the absorption peak height to the background Drude conductivity. Writing the latter as $\sigma_D(\omega) = e^2 G_s G_v \nu_F D/(1 - i\omega\tau)$ with diffusion constant $D = v_F^2 \tau (1 + F_0^d)/2$, we can express the ratio of the resonant to Drude parts of the conductivity as

$$\frac{\text{Re } \sigma_{\text{res}}(\omega = \omega_i)}{\text{Re } \sigma_D(\omega = \omega_i)} \approx \frac{1 + (\omega_i \tau)^2}{2} \frac{\tilde{\alpha}_R^2}{v_F^2} \frac{\tau_s}{\tau} \frac{W_i}{1 + F_0^d}, \tag{25}$$

where W_i is the weight of the δ function for a resonant mode, cf. Eqs. (22) and (24). The ratio τ_s/τ_p, extracted from weak antilocalization measurements in graphene on TMD, varies among different studies [9,27–30]. To be specific, we take $\tau_s \sim \tau \sim 1\,\text{ps}$ [28]. Then the resonant contribution is enhanced by applying a strong in-plane magnetic-field ($H_0 > 10\,\text{T}$) and by choosing a material with larger $\tilde{\alpha}_R$. From the beatings of Shubnikov–de Haas oscillations in bilayer graphene on WSe_2 one extracts $\lambda_R = 10$–$15\,\text{meV}$ [9]; then $\tilde{\alpha}_R/v_F \sim \lambda_R/E_F \sim 0.1$.

To conclude, in this Letter we have shown that in the presence of an external magnetic field the normally diffusive spin-valley modes of graphene evolve into well-defined oscillatory modes with frequency set by the Larmor frequency, and Landau-Fermi-liquid parameters, see Eq. (20). The modes are a generalization of the Silin mode to multivalley materials. They can be probed via EDSR in the presence of extrinsic spin-orbit coupling. Furthermore, certain modes may be selectively excited by changing the polarization of applied E fields, leading to anisotropy of the optical conductivity, see Eqs. (22)–(24).

Acknowledgments. We acknowledge discussions with H. Bouchiat, A. Kumar, S. Maiti, J. Meyer, O. Starykh, and T. Wakamura. This work was supported by NSF Grant No. DMR-2002275 (L.I.G.), Grant No. DMR-1720816 (D.L.M.), and the Yale Prize Postdoctoral Fellowship in Condensed Matter Theory (Z.M.R.). We acknowledge the hospitality of KITP UCSB, supported by NSF Grant No. PHY-1748958, (L.I.G. and D.L.M.) and LPS, University Paris-Sud, Orsay, France (D.L.M.).

[1] E. M. Lifshitz and L. P. Pitaevskii, *Statistical Physics. Part 2. Theory of the Condensed State*, reprinted ed., Course of Theoretical Physics (Elsevier, Oxford, 2006), Vol. 9, p. 387.

[2] V. P. Silin, Oscillations of a Fermi-liquid in a magnetic field, Sov. Phys. JETP **6**, 945 (1958).

[3] P. M. Platzman and W. M. Walsh, Fermi-Liquid Effects on Plasma Wave Propagation in Alkali Metals, Phys. Rev. Lett. **19**, 514 (1967).

[4] S. Schultz and G. Dunifer, Observation of Spin Waves in Sodium and Potassium, Phys. Rev. Lett. **18**, 283 (1967).

[5] D. Candela, N. Masuhara, D. S. Sherrill, and D. O. Edwards, Collisionless spin waves in normal and superfluid ^{3}He, J. Low Temp. Phys. **63**, 369 (1986).

[6] F. Baboux, F. Perez, C. A. Ullrich, I. D'Amico, G. Karczewski, and T. Wojtowicz, Coulomb-driven organization and enhancement of spin-orbit fields in collective spin excitations, Phys. Rev. B **87**, 121303(R) (2013).

[7] F. Baboux, F. Perez, C. A. Ullrich, G. Karczewski, and T. Wojtowicz, Electron density magnification of the collective spin-orbit field in quantum wells, Phys. Rev. B **92**, 125307 (2015).

[8] Z. M. Raines, V. I. Fal'ko, and L. I. Glazman, Spin-valley collective modes of the electron liquid in graphene, Phys. Rev. B **103**, 075422 (2021).

[9] Z. Wang, D.-K. Ki, J. Y. Khoo, D. Mauro, H. Berger, L. S. Levitov, and A. F. Morpurgo, Origin and Magnitude of 'Designer' Spin-Orbit Interaction in Graphene on Semiconducting Transition Metal Dichalcogenides, Phys. Rev. X **6**, 041020 (2016).

[10] E. I. Rashba, Combined resonance in semiconductors, Sov. Phys.-Usp. **7**, 823 (1965).

[11] E. I. Rashba and A. L. Efros, Orbital Mechanisms of Electron-Spin Manipulation by an Electric Field, Phys. Rev. Lett. **91**, 126405 (2003).

[12] M. Duckheim and D. Loss, Electric-dipole-induced spin resonance in disordered semiconductors, Nat. Phys. **2**, 195 (2006).

[13] S. Maiti, M. Imran, and D. L. Maslov, Electron spin resonance in a two-dimensional Fermi liquid with spin-orbit coupling, Phys. Rev. B **93**, 045134 (2016).

[14] I. L. Aleiner, D. E. Kharzeev, and A. M. Tsvelik, Spontaneous symmetry breaking in graphene subjected to an in-plane magnetic field, Phys. Rev. B **76**, 195415 (2007).

[15] M. Kharitonov, Phase diagram for the N=0 quantum Hall state in monolayer graphene, Phys. Rev. B **85**, 155439 (2012).

[16] See Supplemental Material at http://link.aps.org/supplemental/10.1103/PhysRevB.105.L201201 for technical details of calculations.

[17] D. Culcer, Y. Yao, and Q. Niu, Coherent wave-packet evolution in coupled bands, Phys. Rev. B **72**, 085110 (2005).

[18] D. Xiao, M.-C. Chang, and Q. Niu, Berry phase effects on electronic properties, Rev. Mod. Phys. **82**, 1959 (2010).

[19] E. Bettelheim, Derivation of one-particle semiclassical kinetic theory in the presence of non-Abelian Berry curvature, J. Phys. A: Math. Theor. **50**, 415303 (2017).

[20] P. Nozieres and D. Pines, *Theory Of Quantum Liquids*, Advanced Books Classics (Avalon, New York, 1999).

[21] G. Baym and C. Pethick, *Landau Fermi-Liquid Theory: Concepts and Applications*, 1st ed. (Wiley, Hoboken, NJ, 1991).

[22] A. Shekhter, M. Khodas, and A. M. Finkel'stein, Chiral spin resonance and spin-Hall conductivity in the presence of the electron-electron interactions, Phys. Rev. B **71**, 165329 (2005).

[23] D. K. Mukherjee, A. Kundu, and H. A. Fertig, Spin response and collective modes in simple metal dichalcogenides, Phys. Rev. B **98**, 184413 (2018).

[24] D. A. Pesin and A. H. MacDonald, Quantum kinetic theory of current-induced torques in Rashba ferromagnets, Phys. Rev. B **86**, 014416 (2012).

[25] A. Manchon and S. Zhang, Theory of spin torque due to spin-orbit coupling, Phys. Rev. B **79**, 094422 (2009).

[26] I. A. Ado, O. A. Tretiakov, and M. Titov, Microscopic theory of spin-orbit torques in two dimensions, Phys. Rev. B **95**, 094401 (2017).

[27] T. Wakamura, F. Reale, P. Palczynski, S. Guéron, C. Mattevi, and H. Bouchiat, Strong Anisotropic Spin-Orbit Interaction Induced in Graphene by Monolayer WS_{2}., Phys. Rev. Lett. **120**, 106802 (2018).

[28] S. Zihlmann, A. W. Cummings, J. H. Garcia, M. Kedves, K. Watanabe, T. Taniguchi, C. Schönenberger, and P. Makk, Large spin relaxation anisotropy and valley-Zeeman spin-orbit coupling in WSe2/graphene/h-BN heterostructures, Phys. Rev. B **97**, 075434 (2018).

[29] T. Wakamura, F. Reale, P. Palczynski, M. Q. Zhao, A. T. C. Johnson, S. Guéron, C. Mattevi, A. Ouerghi, and H. Bouchiat, Spin-orbit interaction induced in graphene by transition metal dichalcogenides, Phys. Rev. B **99**, 245402 (2019).

[30] Z. Wang, D.-K. Ki, H. Chen, H. Berger, A. H. MacDonald, and A. F. Morpurgo, Strong interface-induced spin-orbit interaction in graphene on Ws2, Nat. Commun. **6**, 8339 (2015).